J Low Temp Phys
DOI 10.1007/s10909-014-1231-4

Transmission Through Gate-Induced Magnetic Islands on Graphene Nanoribbons

R. M. Guzmán Arellano · Gonzalo Usaj

Received: 4 August 2014 / Accepted: 10 September 2014

Abstract We study the spin-dependent transmission through a potential barrier in a zigzag graphene nanoribbon. In particular, we consider the effect of the magnetic order of the ribbon induced by the modulation of the local density introduced by the barrier. We model the system using an Anderson–Hubbard model that we treat in the mean field approximation. We solve this problem self-consistently and calculate the transmission coefficient using the recursive Green function method. We find that Fano-like interference dips appear on one of the spin channels as the result of the presence of spin polarized edge states in the barrier.

Keywords Graphene · Spin-dependent transport · Nanoribbons

1 Introduction

Since the early stages of graphene research, it has been recognized that graphene ribbons with zigzag termination may present spin-polarized states [1]. The magnetic instability arises from the presence of a flat band near the Dirac point. Such a band originates from edge states that are strongly localized [2,3]. The presence of such magnetic order has been studied using different approaches, such as Density Functional Theory (DFT) calculations [4–6], Quantum Monte Carlo, and exact diagonalization [7] or simply using a mean field approximation of the Anderson–Hubbard model [8–10].

In all cases, the results are similar provided the e–e interaction is assumed to be relatively weak ($U \lesssim t$, in the Anderson–Hubbard model language, see below). The nature of the magnetic order, whether the spin polarization at the edges of the ribbons

R. M. Guzmán Arellano (✉) · G. Usaj
Centro Atómico Bariloche and Instituto Balseiro, Comisión Nacional de Energía Atómica and CONICET, San Carlos de Bariloche, Rio Negro, Argentina
e-mail: guzmanar@cab.cnea.gov.ar

Published online: 23 September 2014

has the same or the opposite orientation, depends on doping, being the antiferromagnetic order the ground state of the neutral nanoribbon [4,8]. While the effect of such magnetic ordering on the transport properties has been extensively discussed in the literature, the interplay between modulated doping, induced by the presence of a gate potential, for instance, and the type of ordering has not been explored that much. Here, we study the electron transport through a graphene nanoribbon with a potential barrier that generates a magnetic interface between the leads and the region of the barrier.

2 Model

The graphene ribbon is described by the following mean field Hamiltonian,

$$H = -t_1 \sum_{\langle i,j\rangle,\sigma} c^\dagger_{i\sigma} c_{j\sigma} - t_2 \sum_{\langle\langle i,j\rangle\rangle,\sigma} c^\dagger_{i\sigma} c_{j\sigma} + \sum_i \left(V_{gi}\, \hat{n}_i + \frac{U}{2} \langle \hat{n}_i \rangle \hat{n}_i - \frac{U}{2} \langle \hat{\mathbf{s}}_i \rangle \cdot \hat{\mathbf{s}}_i , \right) \tag{1}$$

where $c^\dagger_{j\sigma}$ ($c^\dagger_{j\sigma}$) is the creation (anhilation) operator for an electron on site j and spin σ, $\hat{n}_i = \sum_\sigma c^\dagger_{i\sigma} c_{i\sigma}$, $\boldsymbol{\tau}$ is a vector operator formed by the Pauli matrices, $\hat{\mathbf{s}}_i = \sum_{\sigma,\sigma'} c^\dagger_{i,\sigma'} \boldsymbol{\tau}_{\sigma'\sigma} c_{i,\sigma}$ is the local spin operator, t_1 (t_2) is the hopping between nearest (next-nearest) neighbors C atoms, U is the Anderson–Hubbard parameter that accounts for the e–e interaction, and V_{gi} is the potential created by the gate electrode at site i. The symbols $\langle \ldots \rangle$ and $\langle\langle \ldots \rangle\rangle$ indicate sum over all sites and their nearest and next nearest neighbors, respectively. Notice that the Hamiltonian (1) admits a non-colinear magnetization [8,9]. In what follows we use $U = 0.77t_1$, $t_2 = 0.1t_1$ and consider a 16 C atoms wide ribbon (8-ZGNR), see Fig. 1a.

3 Results

Firstly, we analyze the case of a uniform ribbon ($V_{gi} = 0$) and calculate the ground state polarization as a function of the graphene's doping δn. Since the largest spin polarization occurs at the edges, we use the angle between the polarizations of the two edges, $\theta = \arccos(\langle \hat{\mathbf{s}}_1 \rangle \cdot \langle \hat{\mathbf{s}}_{16} \rangle / |\langle \hat{\mathbf{s}}_1 \rangle| |\langle \hat{\mathbf{s}}_{16} \rangle|)$, to characterize the magnetic order.

Figure 1b shows θ as a function of the doping δn (excess electrons per unit cell of the ribbon). Clearly, a canted phase is more stable as soon as $\delta n > 0$ (this is consistent with DFT results [11]), while the ferromagnetic phase becomes stable for $\delta n > \delta n_c$. In all this range, the magnitude of the edge magnetization remains approximately constant, $|\mathbf{m}_1| \approx 0.25 \mu_B$. This is shown in Fig. 1c, where the profile of the magnetization along the width of the ribbon is plotted as a function of the doping. The numerical results for θ (dots in Fig. 1b) can be fitted (line) with $\theta = \pi \sqrt{1 - \delta n / \delta n_c}$ with $\delta n_c \sim 0.055$. The ferromagnetic phase remains stable for larger doping, with the edge magnetization gradually vanishing, up to a point (not shown) where the systems become nonmagnetic.

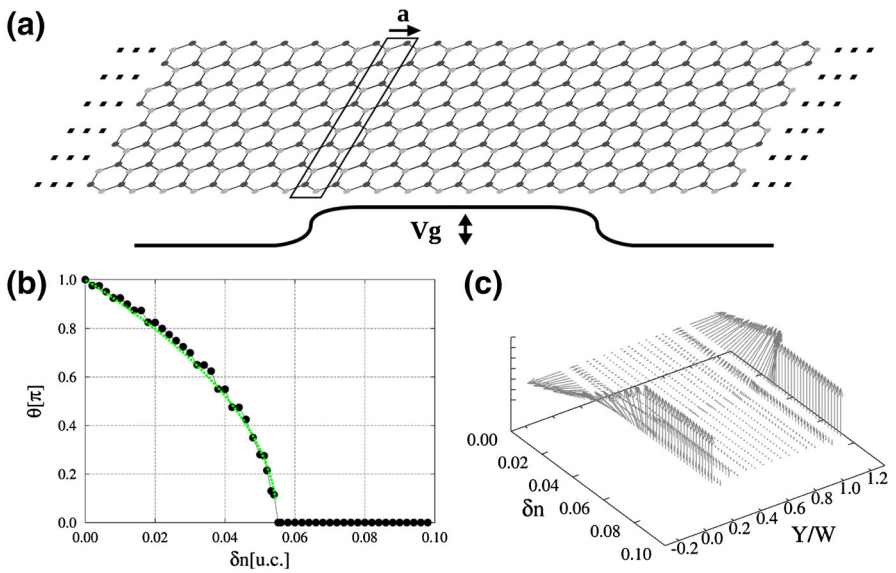

Fig. 1 **a** Scheme of the graphene nanoribbon and the gate potential considered in this work. The unit cell of the ribbon with lattice parameter a is indicated. **b** Angle θ between the polarization of the edges of the ribbon (see text) as a function of the electron doping of the unit cell δn. **c** Magnetization profile along the width of the ribbon as a function of δn (Color figure online)

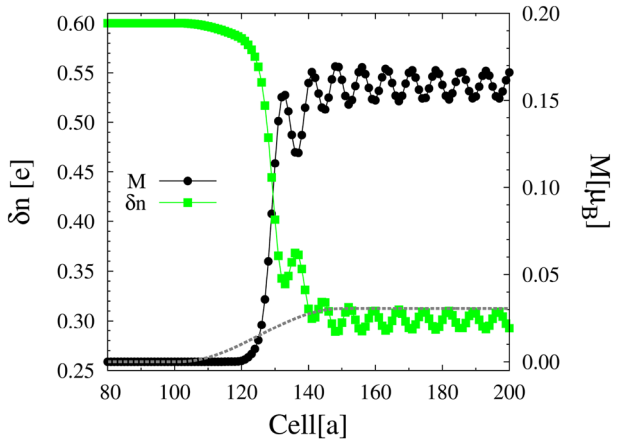

Fig. 2 Spatial dependence of the local electron doping δn (*squares*), the edge magnetization (*dots*) and the gate potential (*thin dashed line*) near the interface between the lead and the gated region (Color figure online)

A spatial modulation of the electron density or doping of the ribbon, and hence of the spin polarization, can be introduced by a non-zero gate potential. Here we analyze the case where the gate potential is such that the local doping deep inside the gated region is $\delta n = 0.3$, and so the ferromagnetic order is favored, while in the lead, the system is nonmagnetic with the doping set to be $\delta n = 0.6$. Figure 2 shows the self-consistent spatial dependence of both the local density and the edge magnetization

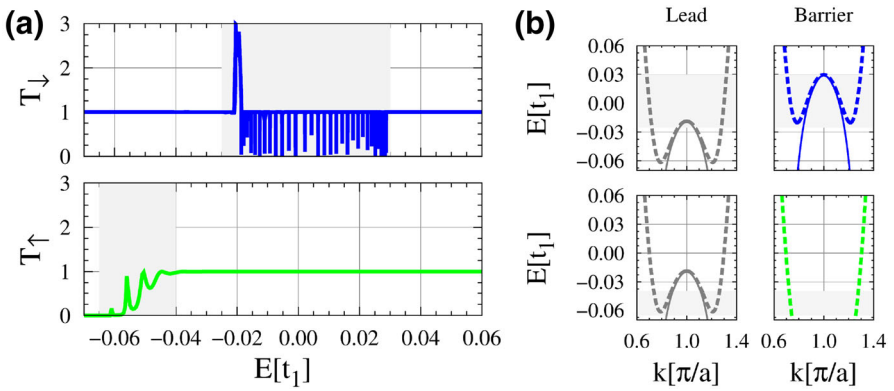

Fig. 3 **a** Spin-dependent transmission as a function of the energy of the incident electron. **b** Band structure of an infinite ribbon with the same electron density as in the leads (*left*) and in the middle of the barrier (*right*) for the two spin cases. *Shadow* areas highlight the energy range where non-trivial effect occurs (Color figure online)

near the interface between the lead and the gated region. Apart from the expected Friedel-like oscillations inside the barrier, the result shows that the barrier leads to a finite spin-polarized region. Notice that the change of the magnetization and the density is more abrupt than the change of the gate potential.

Once the self-consistency is obtained, we can calculate the conductance in the linear response regime using the Landauer approach. For that, we use the standard procedure to obtain the transmission coefficient T from the Green function of the system.

Figure 3a shows the transmission as a function of the energy and the spin of the incident electron, $T_\uparrow$ and $T_\downarrow$. There is a clear difference between the two spin orientations. To understand this behavior we plot in Fig. 3b the spin-dependent bands of an infinite ribbon with an electron density per unit cell corresponding to the one of the leads (left panels) or to the one at the center of the gated region (right panels). We then assume that these bands are a good description of the states in the leads and deep inside the barrier and so the main features of the transmission can be understood in terms of matching conditions between these states. Since the leads are paramagnetic, the allowed states are the same for both spins: in the energy range shown in the figure, there is only one incident transverse channel slightly above $E \sim -0.02t_1$ and there are three channels below it. The bands plotted with thick dashed (thin solid) lines have an even (odd) parity with respect to the center of the ribbon. This is important as parity conservation imposes a restriction on the transmission through the potential barrier. The 'bands' associated to the barrier states, on the other hand, have the following characteristics and the corresponding effects on transport: (i) *spin up case* there is a single featureless band of even parity. Because there is a single available channel inside the barrier and it matches well with the even lead states, the transmission is very close to one in almost all the energy span—except near the minimum of the even lead band where the states with $k \in [0.8\pi/a, 1.2\pi/a]$ are edge states [10] (ii) *spin down case* below $E \sim -0.02t_1$, there is an odd band that couples well with the lead channels leading to essentially perfect transmission. Above that energy there is no odd channel in the leads and so these states do not participate in the transport. Above

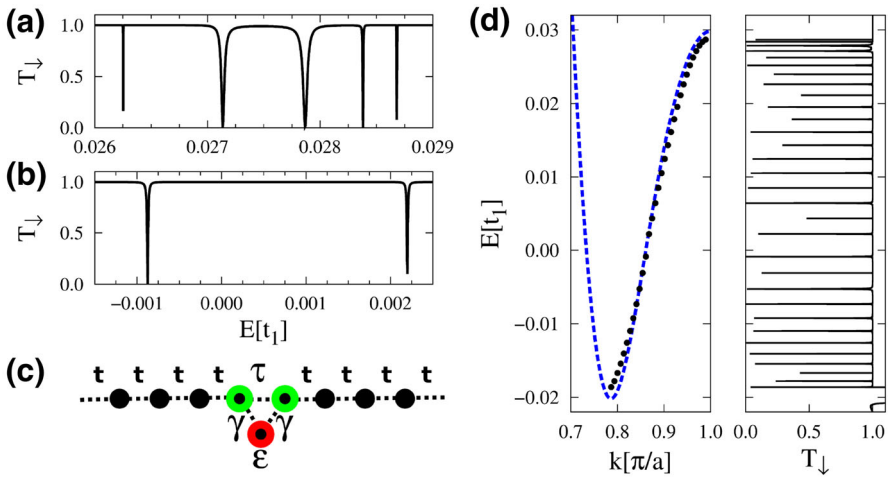

Fig. 4 **a**, **b** Transmission of down electrons in two different energy ranges that show Fano dips of different shapes. **c** Scheme used to interpret the data (see text). **d** Comparison of the position of the resonant energies ($\varepsilon_n(k_n)$) with the band associated to the states inside the barrier (Color figure online)

$E \sim 0.03t_1$ the same happens, but with an even band involved. However, the even band contains two channels in the energy range between these two cases (shadowed area in the figure): the ones with $k \in [0.8\pi/a, 1.2\pi/a]$, which are edge states [2,10], and the ones outside that range, which are extended states (in the transverse direction) as the lead modes. Both channels couple to the leads but in very different way leading to interference effects that produce dips in the transmission as we explain below.

Figures 4a, b show $T_\downarrow$ in two different energy ranges in more detail inside the region where the transmission present dips. These dips, that reach zero transmission at their centers, can be understood as the interference between a transmission channel with a continuous spectrum and a resonant channel (the well known Fano effect [12,13]).

A scheme of a model that contains this physics is shown in Fig. 4c. In our case, the continuous channel is represented by the extended states of the even mode inside the barrier, which are strongly coupled to the leads (τ hopping in the model) and thus providing a channel with $T \sim 1$. The role of the resonant states (with energy ε) is played by the edge states inside the barrier, which are weakly coupled to the leads ($\gamma \ll t, \tau$) due to the small overlap between these states and the extended lead states. This very simple model can explain a dip in the transmission as the result of the interference between the two transmission paths. In addition, the different shapes of the dips can be understood from the fluctuations on the values of the model effective parameters, which in the actual system arise from details of the wave function matching between states in the leads and inside the barrier.

The reason why there are many resonant states can be found in the fact that these edge states can be thought as having a discrete spectrum due to the confinement induced by the magnetization profile. Indeed, if we assume that the confinement is given by the length L of the region with non-zero magnetization, we expect that the confined state will have a wave-vector $k_n \simeq n\pi/L + k_0$, where n is an integer number and k_0 a correction to the hard wall confinement. The position of the resonances (ε_n)

will depend on the exact form of the energy dispersion and it is difficult to evaluate. Nevertheless, to show that this interpretation makes sense, we extracted the position of the Fano resonances in the transmission and plot them as a function of k_n assuming that the resonance at the highest energy corresponded to $n = 31$ and taking $k_0 = 0.78\pi/a$ and $L = 150a$, the former parameter was chosen to fit the band and the latter taken from the data in Fig. 2. This is shown in Fig. 4d and compared with the band for down spins of a system with the same density as in the middle of the barrier. There is a very good agreement that supports our interpretation.

4 Conclusions

We have shown that local gating in graphene ribbons can lead to strong fluctuation of the spin-dependent transmission coefficient. This originates from the fact that local gating can induce changes in the local magnetic order of the ribbon. In particular, in the case of a ferromagnetic barrier, we showed that the presence of edge states with a poor matching with the lead states generates Fano-like dips in the transmission. If the Fermi energy falls near one of these dips, the current will be strongly polarized. Even though we have presented results only for a 8-ZGNR, our results extend to wider ribbons. One can envision that more exotic interfaces with different magnetic domains might be possible, but that is beyond the scope of the present work. The recently developed technique to grown high quality ribbons with atomically defined edges [14] might open the door to study this type of magnetic effects on transport.

Acknowledgments We acknowledge financial support from PICT Bicentenario 2010-1060 from ANPCyT, PIP 11220080101821 and 11220110100832 from CONICET and 06/C415 SeCyT-UNC.

References

1. A.H. Castro Neto, F. Guinea, N.M.R. Peres, K.S. Novoselov, A.K. Geim, Rev. Mod. Phys. **81**, 109 (2009)
2. L. Brey, H.A. Fertig, Phys. Rev. B **73**, 235411 (2006)
3. K. Sasaki, S. Murakami, R. Saito, Appl. Phys. Lett. **88**, 113110 (2006)
4. Y.-W. Son, M.L. Cohen, S.G. Louie, Nature **444**, 347 (2007)
5. S.M.-M. Dubois, Z. Zanolli, X. Declerck, J.C. Charliera, Eur. Phys. J. B **72**, 1 (2009)
6. L. Yang, C.H. Park, Y.-W. Son, M.L. Cohen, S.G. Louie, Phys. Rev. Lett. **99**, 186801 (2007)
7. H. Feldner, Z.Y. Meng, A. Honecker, D. Cabra, S. Wessel, F.F. Assaad, Phys. Rev. B **81**, 115416 (2010)
8. J. Jung, A.H. MacDonald, Phys. Rev. B **79**, 235433 (2009)
9. J. Jung, A.H. MacDonald, Phys. Rev. B **81**, 195408 (2010)
10. G. Usaj, Phys. Rev. B **80**, 081414(R) (2009)
11. K. Sawada, F. Ishii, M. Saito, S. Okada, T. Kawai, Nano Lett. **9**(1), 269 (2009)
12. U. Fano, Phys. Rev. **124**, 1866 (1961)
13. H.M. Pastawski, E. Medina, Rev. Mex. Fis. **47**(S1), 1 (2001)
14. J. Baringhaus, M. Ruan, F. Edler, A. Tejeda, M. Sicot, A. Taleb-Ibrahimi, A. Li, Z. Jiang, E.H. Conrad, C. Berger, C. Tegenkamp, W.A. de Heer, Nature **506**, 349 (2014)